Long-Haul WDM Transmission Using Higher Order Fiber Dispersion Management

M. Murakami, T. Matsuda, H. Maeda, and T. Imai

***Abstract*—We propose a fiber dispersion management scheme for large-capacity long-haul wavelength division multiplexing (WDM) transmission systems that considers not only second- but also third-order dispersion characteristics using transmission fibers with opposite dispersion signs. It eliminates the waveform distortion of WDM signals that originates from the existence of third-order dispersion, which is a constraint placed on WDM capacity in conventional dispersion management, while reducing the interchannel interaction caused by the interplay of fiber nonlinearity and second-order dispersion. Design concept of the scheme is discussed to show the feasibility of using actual fiber parameters. An experimental investigation on transmission performance regarding the signal pulse format, nonreturn-to-zero (NRZ) and return-to-zero (RZ), and interchannel interaction caused by four-wave mixing (FWM) and cross-phase modulation (XPM) is described for optimizing WDM system performance. It is experimentally shown that RZ pulse transmission is possible without significant spectral broadening over a wide wavelength range in dispersion managed fiber spans. Using these results together with a wideband optical amplifier gain-bandwidth management technique, yields long-distance WDM transmission with the capacity of 25 $\times$ 10 Gb/s over 9288 km.**

***Index Terms*—Optical amplifiers, optical fiber cables, optical fiber communication, optical fiber dispersion, optical Kerr effect.**

I. Introduction

RECENT developments in wavelength division multiplexing (WDM) technology offer transmission capacities that exceed those of single-channel time division multiplexing (TDM) systems. Indeed, large-capacity long-haul WDM transmission systems over transoceanic distances are now being intensely studied for installation. The transmission capacity of WDM systems can be increased by raising the signal bit rate per channel and/or the number of signal channels. In terms of realizing terminal equipment, increasing the number of channels seems easier than increasing the signal bit rate. This is because increasing the signal bit rate requires the development of higher speed electronic circuits and optical devices, while increasing the number of channels can be achieved by simply modifying the optical circuits. Therefore, the number of signal channels is rapidly growing in WDM systems [1].

The number of signal channels depends on the available optical passband width of the system as well as the channel spacing, so that increasing the available optical passband width is essential for increasing the transmission capacity of WDM systems. This is mainly determined by the optical fiber characteristics such as dispersion and nonlinearity, as well as the gain bandwidth of optical amplifiers. In particular, long-haul systems are significantly impacted by the interplay between fiber dispersion and nonlinearity, so very careful consideration of the dispersion characteristics is needed [2].

Fiber nonlinearity and dispersion are known to cause signal waveform distortion and interchannel interaction between WDM signals [3]. Waveform distortion, which is due to the interplay between self-phase modulation (SPM) and dispersion, can be reduced by decreasing the value of dispersion. This value mainly depends second-order-dispersion, i.e., group velocity dispersion (GVD). To the contrary, interchannel interaction, which is due to cross-phase modulation (XPM) or four-wave mixing (FWM), becomes smaller as GVD value increases.

Conventional WDM systems resolved this conflict by using nonzero dispersion fibers to achieve large local GVD and inserting dispersion compensators at regular intervals to eliminate GVD over the entire system. Such configuration successfully reduces both the interchannel interaction and the signal waveform distortion caused by the interplay of fiber nonlinearity and GVD.

Such an approach, however, manages only second-order dispersion, so signal channels that deviate from the average zero-dispersion wavelength (ZDW) experience dispersion accumulation along the entire system length because of the existence of higher order dispersion. This accumulated dispersion leads to waveform distortion in those signal channels due to the interplay with SPM and the distortion becomes more significant with the channel bit rate. Thus, the existence of higher order dispersion limits the available passband width of the WDM system in terms of fiber characteristics. This restriction has become critical given recent demands for long-haul WDM systems with SDH data rates of 10 Gb/s or more [2], [4].

Using transmission fibers with opposite dispersion signs is one approach to reduce third-order dispersion [5]. Indeed, simply combining such fibers that have exactly the same level of dispersion could reduce third-order dispersion and transmit all WDM signals without dispersion compensation over a few hundred kilometers [6]. However, such a primitive configuration is ineffective for long-haul transmission systems with transoceanic distances, because they suffer from intense fiber nonlinear effects and critically depend on dispersion allocation [2].

This paper proposes a dispersion management technique suitable for long-haul WDM systems that covers both second- and third-order dispersion characteristics of the system and suppresses both waveform distortion and interchannel interaction. The outline and design technique of the dispersion

Manuscript received January 4, 2000; revised May 30, 2000.

The authors are with NTT Network Service Systems Laboratories, Kanagawa 238-0847, Japan.

Publisher Item Identifier S 0733-8724(00)08070-1.

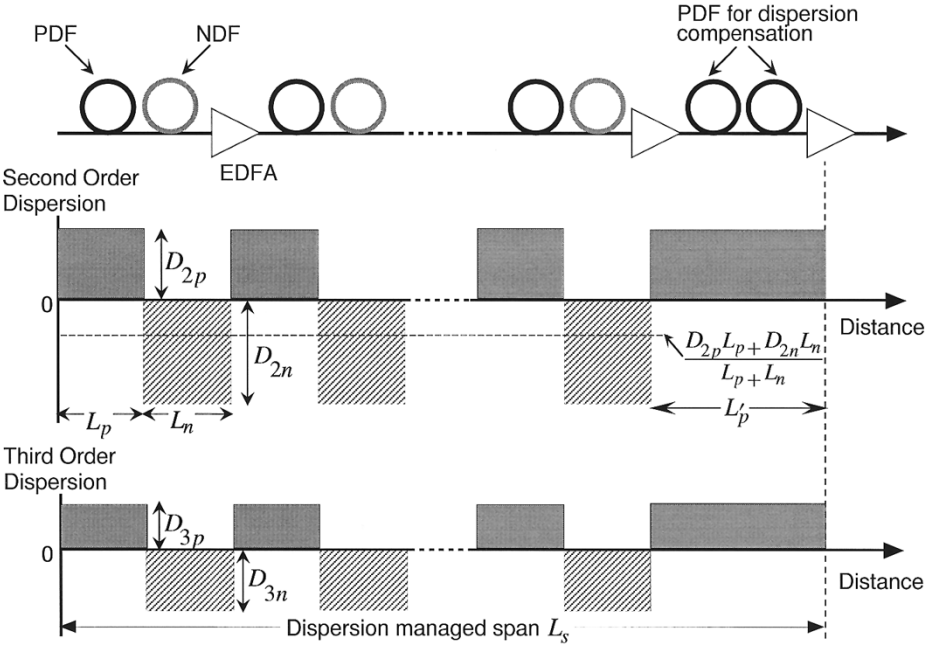

Fig. 1. Proposed second- and third-order fiber dispersion management scheme that uses positive-dispersion fibers (PDFs) and negative-dispersion fibers (NDFs).

management scheme is described in Section II. Section III investigates single-channel transmission performance with reference to pulse format, nonreturn-to zero (NRZ) and return-to zero (RZ). It is experimentally shown that such a dispersion managed transmission line has a unique RZ signal transmission characteristic that is unlike that seen with linear pulse propagation. Section IV describes experimental results on interchannel interaction due to fiber nonlinearity in the dispersion managed transmission line. These results, together with wideband optical gain equalization and reduction in third order dispersion to one-tenth that of the conventional value, realize WDM transmission of 25 channel 10 Gb/s signals over 9288 km as is shown in Section V.

II. High Order Fiber Dispersion Management Scheme

The proposed dispersion arrangement, which considers both the second- and third-order dispersion characteristics, is illustrated in Fig. 1. Each repeater span basically consists of two kinds of fibers; one has positive second- and third-order dispersion values [positive-dispersion fiber (PDF)] and the other has negative values [negative-dispersion fiber (NDF)]. Both the second- and third-order dispersion characteristics of the system should be simultaneously managed to realize transoceanic distance transmission.

For second order dispersion control, we arrange the PDF (dispersion value is D_{2p}, length is L_p) and NDF (D_{2n} and L_n) so that the subtotal of their product in each repeater span, i.e., $L_pD_{2p}+L_nD_{2n}$, is not zero but remains a constant value. This is because the local second-order dispersion value should be as large as possible to reduce the interchannel interaction caused by fiber nonlinearity as is the case in the conventional scheme.

The second-order dispersion accumulated over several repeater spans (the sum total of each $L_pD_{2p}+L_nD_{2n}$) is then compensated by a set of positive-dispersion fibers inserted at a predetermined dispersion compensation interval, $\hat{L}_s$. As a result, the second-order dispersion value in the unit dispersion management span, L_s is forced to zero. This is because the average value should be small to avoid the waveform distortion caused by the interaction between SPM and dispersion.

If $\hat{L}_s$ is composed of M spans of sets of PDF and NDF, and the length of PDF for dispersion compensation is given by L'_p, then the second-order dispersion value of the unit dispersion management span is expressed by the following relationship:

$$D_{2S}=\frac{D_{2p}(ML_p+L'_p)+MD_{2n}L_n}{L_S}. \tag{1}$$

On the other hand, the second-order dispersion value before compensation is given by

$$\hat{D}_{2S}=\frac{M(D_{2p}L_p+D_{2n}L_n)}{\hat{L}_S}=\frac{D_{2p}L_p+D_{2n}L_n}{L_p+L_n} \tag{2}$$

which would typically be minus a few ps/nm/km for effective suppression of interchannel interaction. Such a combination of PDFs and NDFs must simultaneously reduce the third order dispersion to the greatest possible extent. Our approach is not to make the third order dispersion zero in each repeater span (i.e., $L_pD_{3p}+L_nD_{3n}\neq 0$) but zero over the unit dispersion management span, L_s, due to the need to achieve the second-order dispersion management above mentioned. The total third-order dispersion value of the span L_s, is given by

$$D_{3S}=\frac{D_{3p}(ML_p+L'_p)+MD_{3n}L_n}{L_S}. \tag{3}$$

Provided that D_{2s} equals zero, we can obtain the following simple expression for D_{3s},

$$D_{3S} = \frac{\dfrac{D_{3p}}{D_{2p}} - \dfrac{D_{3n}}{D_{2n}}}{\dfrac{1}{D_{2p}} - \dfrac{1}{D_{2n}}} = \frac{R_p - R_n}{\dfrac{1}{D_{2p}} - \dfrac{1}{D_{2n}}} \tag{4}$$

where R_p and R_n mean the ratio of third- to second-order dispersion values for PDFs and NDFs, respectively. Equation (4) suggests that the third-order dispersion value over the entire system is mainly determined by the miss-match between R_p and R_n of both kinds of fiber.

Fig. 2 shows the calculation result for the third-order dispersion value of the unit dispersion management span normalized by that of the PDF, D_{3s}/D_{3p} against the dispersion miss-match factor, R_n/R_p with different values of D_{2n}/D_{2p}. We can see that the absolute value of D_{3s}/D_{3p} linearly increases as R_n/R_p. deviates from one, and that its behavior depends on D_{2n}/D_{2p}. For example, D_{3s} can be reduced to 1/10 of D_{3p} if R_n/R_p ranges between 0.8–1.2 for the case $D_{2n}/D_{2p} = 1$.

In our experiment, the PDFs used were so-called single-mode fibers. The NDFs were designed to match the PDFs in each repeater span in terms of second- and third-order dispersion, unlike the conventional dispersion compensation fibers (DCFs). We located the PDF ahead of the NDF in each repeater span to reduce the fiber nonlinear effects because the PDF has a larger mode-field diameter, typically 9–10 μm, than the NDF. We also note that its mode field diameter is larger than that of typical conventional dispersion-shifted fibers (DSFs).

The effect of fiber nonlinearity and dispersion is generally described by using the "characteristic length" [3]. Waveform distortion caused by SPM and second-order dispersion depends on the product of nonlinear length and dispersion length [7], [8]. To suppress significant waveform distortion, the lengths of positive and negative fibers, L_p and L_n, should satisfy the following relationship:

$$L_p \le \sqrt{L_{D2p} L_{NLp}} \tag{5}$$

$$L_n \le \sqrt{L_{D2n} L_{NLn}} \tag{6}$$

where L_{D2} and L_{NL} are dispersion length and nonlinear length for either kind of fiber, respectively.

To reduce the interchannel interaction due to XPM effectively, dispersion compensation interval, $\hat{L}_s$ should be sufficiently longer than the walk-off length L_W, which is determined by the signal pulse width, channel spacing, and second-order dispersion [2], [3]. On the other hand, $\hat{L}_s$ must be shorter than the square root of the product of nonlinear length and dispersion length as is true for L_p and L_n. These relationships are expressed as

$$L_w \le \hat{L}_S \le \sqrt{L_{\hat{D}2s} L_{N\hat{L}_s}}. \tag{7}$$

Using (1)–(7), yields the fiber arrangement in a higher-order dispersion management transmission line.

In what follows, we calculate these lengths for a system with typical parameters; the signal has a Gaussian pulse shape with a full-width at half-maximum (FWHM) of 100 ps (NRZ), fiber

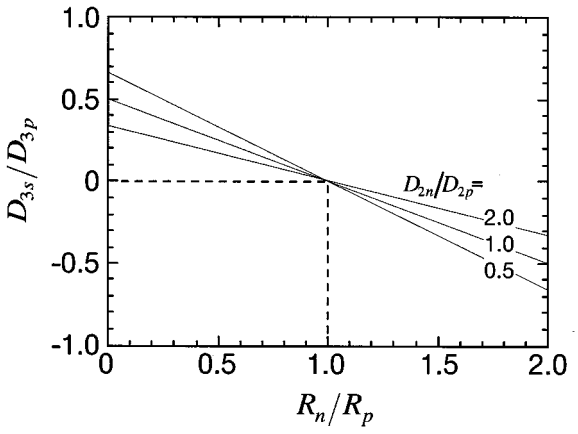

Fig. 2. Third-order dispersion value of the entire transmission line normalized by that of the PDF (D_{3s}/D_{3p}) versus second- and third-order dispersion ratio miss-match between PDF and NDF (R_n/R_p) for the second-order dispersion ratios between PDF and NDF (D_{2n}/D_{2p}) of 0.5, 1, and 2.

nonlinear coefficient is 3.2×10^{-20}m^2/W. If PDF has the effective core area of 66 μm^2 and the second-order dispersion of 17 ps/nm/km, $\sqrt{L_{D2p} L_{NLp}}$ becomes 357 km when path-averaged signal peak power is 0.7 mW. On the other hand, for NDF, $\sqrt{L_{D2n} L_{NLn}}$ is 258 km, given the effective core area is 21 μm^2, second-order dispersion is 27 ps/nm/km, and path-averaged signal peak power is 0.25 mW. With RZ signal pulses, these lengths are simply reduced by a factor of $\sqrt{8}$ because they have half the pulse width of NRZ signal pulses and twice the signal peak power if the average optical power is the same. These results suggest that we can configure each repeater span, typical length of which ranges less than several tens of km, with a set of PDF and NDF.

If we assume the channel spacing is 0.8 nm and $\hat{D}_{2S}$ is -2 ps/nm/km, L_W is calculated to be 37.5 km for NRZ pulses; the value is halved for RZ pulses. Provided that each repeater spacing consists of PDF and NDF (each 20 km long) in addition to the above parameters, $\sqrt{L_{\hat{D}2s} L_{N\hat{L}_s}}$ equals 998 km. These results allow us to realize the proposed dispersion managed span with realistic parameters.

III. Single-Channel Transmission Experiment

We measured the single-channel transmission performance of a dispersion managed line. The experimental configuration of the recirculating loop setup is shown in Fig. 3. In the transmitter, an intensity-modulator generated $2^7 - 1$ pattern NRZ or RZ signals with the data rate of 10 Gb/s. The RZ pulse format had a duty ratio of 50%.

The 362-km length loop consisted of erbium-doped optical amplifiers (EDFAs), each pumped by a 980 nm laser, transmission fibers, and an optical filter to manage the optical amplifiers' passband. The typical repeater span length between the EDFAs was 40 km (20 km of which consisted of PDF). The typical second- and third-order dispersion values of the PDFs were $+17$ ps/nm/km and 0.06 ps/nm^2/km, respectively. The values of the NDFs were -27 ps/nm/km and -0.06 ps/nm^2/km, respectively. We arranged the fibers so that the average of their second-order dispersion values ranged around -3 ps/nm/km in

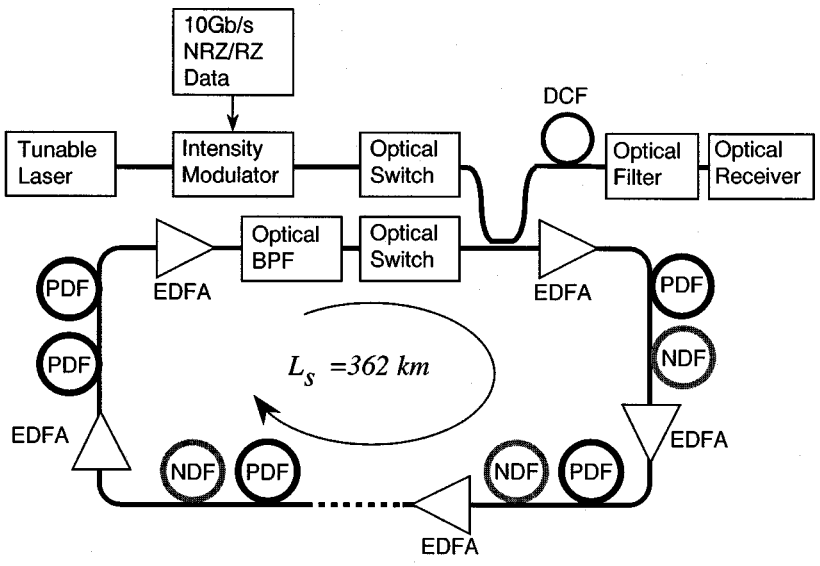

Fig. 3. Experimental setup for single-channel transmission.

each repeater span. The accumulation of this second-order dispersion was offset to zero using a set of PDFs. We placed the PDF ahead of the negative one in each repeater span since the former had a larger mode-field diameter (9.2 mm) than the latter (5.7 mm).

The output power from each EDFA was set to around -3 dBm. The power of the recirculating signal was tapped and one of signal channels was selected by an optical filter with a bandwidth of 0.4 nm, for detection by the optical receiver. The DCF ahead of the receiver was used to compensate the accumulated second-order dispersion for each signal channel caused by the residual third-order dispersion that could not be canceled in the loop.

Fig. 4 shows the relative group delay and dispersion characteristics measured for the entire 362-km loop length. We find that the third-order dispersion was successfully reduced to 0.013 ps/nm^2/km at the measured wavelength range, about 1/6 that of a typical DSF, while second-order dispersion was set to zero at 1545.8 nm.

We measured the single-channel transmission performance of the NRZ and RZ pulse formats at the ZDW. Fig. 5 shows the electrical signal-to-noise ratio (SNR) against transmission distance. The electrical SNR is related to the so-called Q-parameter in that it is four times of the Q^2 value [9], [10]. It was estimated by measuring the bit error rate while sweeping the decision threshold level of the receiver [11]. We find that the electrical SNR is, basically, inversely proportional to distance, that is, according to the amplifier noise accumulation, for both formats; the saturation arising in the relatively large SNR region was suppressed for the pattern length used. We note that RZ pulses yield larger SNR than NRZ pulses for the distances examined. This is because RZ pulses have larger signal peak power, and so have larger eye opening than NRZ pulses for the same optical amplifier output power. Moreover, RZ pulses offer the advantage of waveform independence from the signal pattern, unlike NRZ pulses. This becomes more significant in a dispersion managed line wherein the interaction between SPM and GVD might periodically compress and stretch the pulse; SPM induces chirping only

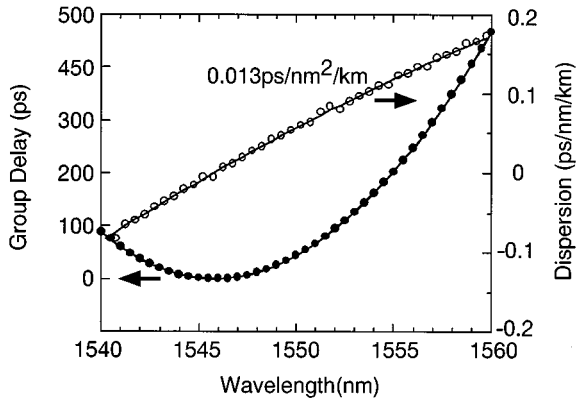

Fig. 4. Measured group delay and dispersion characteristics for 362 km amplifier-fiber chain.

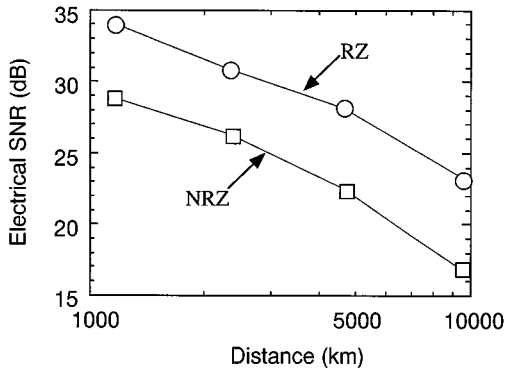

Fig. 5. Electrical SNR versus distance measured for single- channel NRZ and RZ transmission.

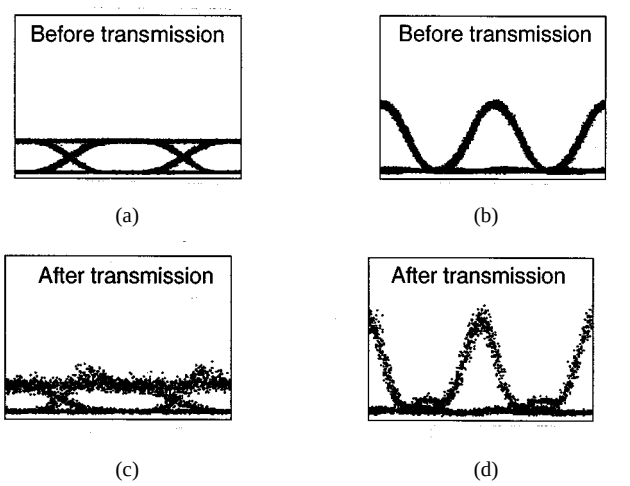

Fig. 6. (a), (c) Signal waveforms for NRZ and (b), (d) RZ formats measured with electrical bandwidth of more than 20 GHz; before transmission (a), (b), after 2172 km transmission (c), (d).

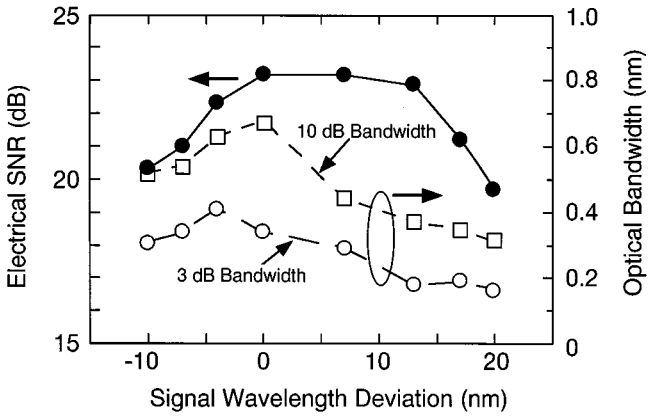

Fig. 7. Electrical SNR and optical bandwidth of single-channel RZ pulse after 9050 km transmission versus wavelength offset from the average ZDW; bandwidth was measured with a resolution of 0.1 nm.

at the leading and falling edges of the signal pulses, while the NRZ pulse waveform depends on the bit pattern. Fig. 6 shows the waveform evolution for NRZ and RZ pulse formats; these were measured with the electrical bandwidth of more than 20 GHz (unlike baseband width). We note that RZ pulses were compressed, which reduced the duty ratio, while NRZ pulses were simply degraded during propagation.

The following investigations consider RZ signal transmission characteristics when the signal wavelength deviates from the zero-dispersion wavelength (ZDW), i.e., for a change in the average dispersion value of the entire transmission line. For situations in which the signal wavelength deviation exceeded the optical passband-width of the EDFAs, we modified the dispersion allocation slightly in addition to changing the absolute signal wavelength. Fig. 7 shows the electrical SNR and optical bandwidth of the signal pulse measured after transmission. The optical bandwidth was measured with a resolution of 0.1 nm. We found that the dependence of the SNR on the separation from the ZDW is not symmetrical but asymmetrical. Larger SNR was achieved in the anomalous dispersion region, in terms of the average characteristic over the transmission line. No significant SNR degradation was observed for wavelength separations of up to 13 nm.

Such a dependency suggests that the pulses transit the transmission line not as linear pulses but are significantly affected by fiber nonlinearity. We consider that the periodic dispersion fluctuation and SPM compress the RZ pulses such that they exhibit soliton-like behavior. Moreover, the pulse broadening was reduced as the signal wavelength diverged from the ZDW in the anomalous dispersion region; SPM does not necessarily broaden the optical spectrum in such a condition. The 3 dB and 10 dB optical bandwidths changed from 0.41 to 0.16 nm and 0.68 to 0.31 nm in the measured wavelength range, respectively. We note that this narrow optical spectrum is satisfactory in WDM systems, because it well suppresses the interchannel crosstalk experienced during optical filtering in front of the receiver. Consequently, the above results indicate that setting most signal wavelengths longer than ZDW yields the best transmission performance in such a dispersion managed line.

IV. Interchannel Interaction

We measured the interchannel interaction between two-channel WDM signals with different channel spacings and polarization coupling states in the dispersion managed line. Experimental set-up was the same as Fig. 3 except for the transmitter configuration. The two wavelength signals were separately intensity-modulated with 10 Gb/s RZ format and coupled with their polarization states parallel or orthogonal to each other. The wavelength of the measured signal channel was set at 1549.3 nm, while ZDW was 1545.8 nm. The channel spacing between the measured signal channel and the interference channel was shifted by sweeping the wavelength of the tunable laser. The EDFA output power was set so that each signal channel power was -3 dBm. In front of the receiver, an optical filter that could suppress the interchannel crosstalk to less than -20 dB for the wavelength separation of 0.3 nm was used to isolate one of the signal channels.

Fig. 8 shows the optical spectra measured after 9050 km transmission for the wavelength spacings of 0.4 nm and 1.2 nm when the polarization state between the signal channels was in parallel. No significant generation of FWM lights was observed for the channel spacing of 1.2 nm and even for 0.4 nm. The reason for this is considered to be that the local GVD values of PDFs and NDFs are relatively large compared to those of conventional DSF such that effective FWM interaction during propagation did not occur even though the channel spacing was narrow and parallel polarization coupling was used.

Fig. 9 shows the electrical SNR measured as a function of channel spacing. The SNR remained basically constant if the channel spacing was wider than 0.4 nm, when the signals had orthogonal polarization states. In contrast, channel spacings narrower than 0.8 nm gave rise to a decrease in SNR with parallel polarization coupling. This difference in SNR behavior might be due to the effect of XPM, which significantly depends on the polarization states between the multiplexed signal channels [3]. Fig. 10(a) and (b) shows the waveforms measured with the channel spacing of 0.3 nm for each polarization coupling state. We note that intense waveform degradation arose when parallel polarization coupling was employed, unlike orthogonal polar-

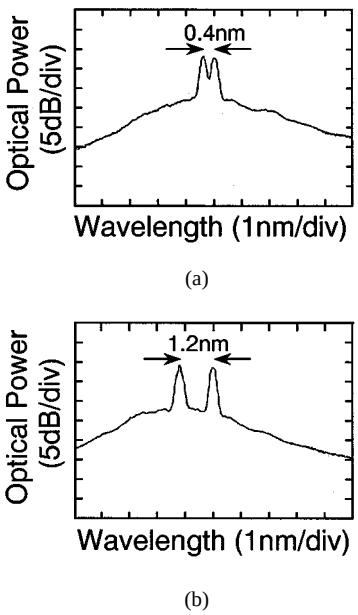

Fig. 8. Optical spectra with channel spacing of (a) 0.4 nm and (b) 1.2 nm for two-channel WDM transmission.

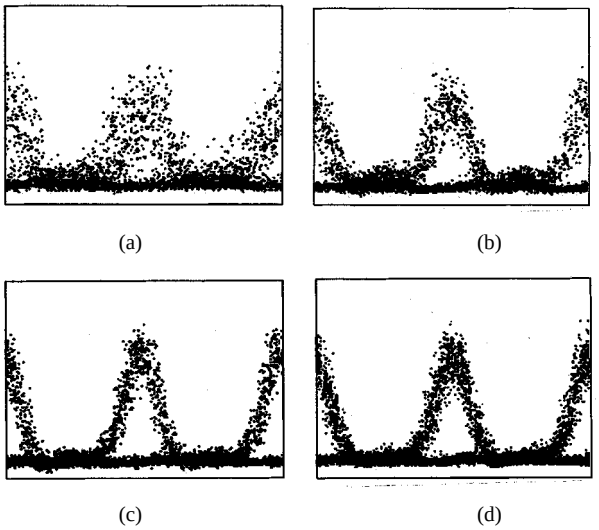

Fig. 10. Signal waveforms measured for two-channel WDM transmission. Channel spacing is 0.3 nm with (a) parallel polarization coupling and (b) orthogonal polarization coupling. Channel spacing is 1.2 nm with (c) parallel polarization coupling and orthogonal (d) polarization coupling.

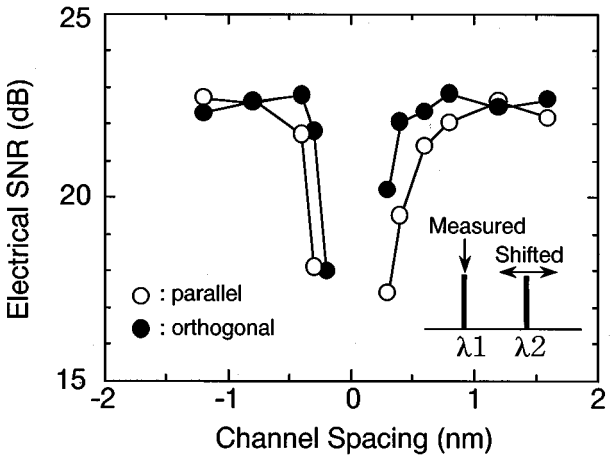

Fig. 9. Measured electrical SNR versus channel spacing for two-channel WDM transmission coupled with parallel and orthogonal polarization states.

ization coupling. In contrast, no significant waveform degradation was observed for either polarization coupling state when the channel spacing was increased to 1.2 nm as shown in Fig. 10(c) and (d). This indicates that XPM was ineffective in terms of creating signal interaction without regard to polarization coupling state given wide channel spacing.

V. Quarter Tb/s WDM Transmission Experiment

WDM transmission was established using the experimental set-up shown in Fig. 11. Twenty-five lasers generated signal wavelengths ranging from 1541.6 to 1558.4 nm with 0.7 nm spacing. Even and odd number channels were separately intensity-modulated with 10 Gb/s, $2^7 - 1$ pattern RZ pulse format with duty ratio of 50%, and the signal pulses in each path were sinusoidally chirped by a phase modulator driven at clock frequency [12]. They were coupled with their polarization states orthogonal to each other to reduce fiber-nonlinearity-induced interchannel interaction, mainly XPM, as was suggested by the results in Section IV. Fig. 12 shows the optical spectrum of the transmitter output. The optical power levels of the signal channels showed less than 0.5 dB deviation and no intentional preemphasis was employed. This is because excessive optical signal power level variation might lead to optical SNR degradation during propagation. The EDFA output power was set at around 12 dBm. The ZDW, averaged over the entire loop, was set at 1541.8 nm taking the results in Section III into account.

In addition to the fiber dispersion characteristics, the gain bandwidth of the optical amplifier cascade should be precisely managed to achieve the optical passband required for WDM transmission. We widened the gain bandwidth by combining several optical equalizers that offered Mach–Zehnder interferometer type response with different free spectral ranges (FSRs) and depths as shown in Fig. 13. The equalizer cascades realized the exact inverse of the response of the EDFA cascades in the loop.

Fig. 14 shows the measured group delay and the optical spectrum after 9288 km propagation. To cover the wide wavelength range of 16.8 nm for WDM transmission, the third order dispersion value was further reduced to 0.0067 ps/nm^2/km, one-tenth the value typical of conventional DSF, by adjusting the dispersion values of the PDFs and NDFs; the loop length was changed to 387 km. The synthesized equalizers successfully widened the available optical passband width to transmit all the signal wavelengths and the signal level difference between the channels was held to under 5 dB. The slight variation in the signal level, the period is of the order of several nm, originates from the fact that gain equalizers can flatten the gain profile only for periods longer than their FSRs. As expected from the result in

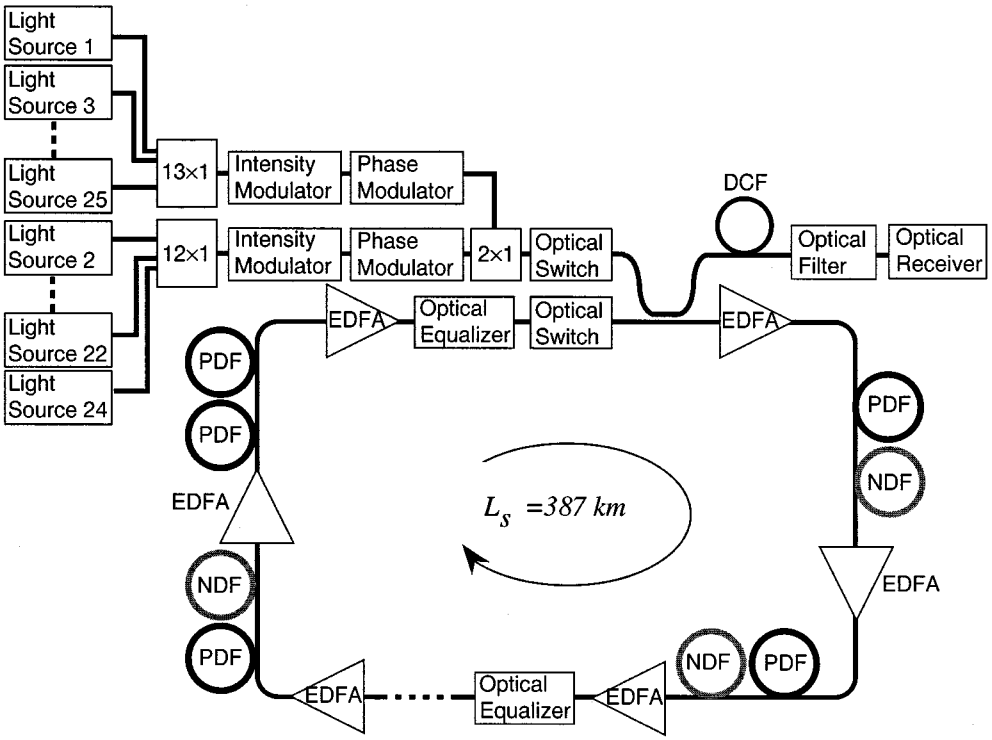

Fig. 11. Configuration of 25 × 10 Gb/s WDM transmission experiment.

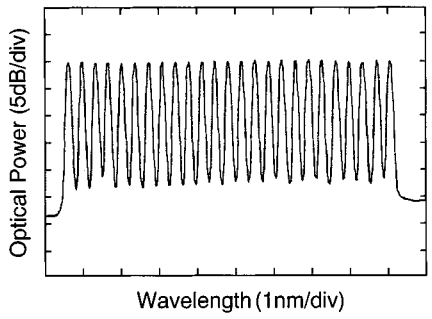

Fig. 12. The optical spectrum of the transmitter output.

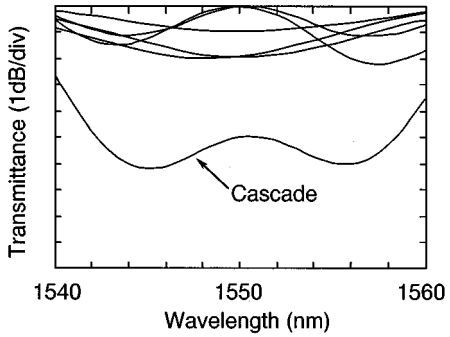

Fig. 13. The spectrum of cascaded optical equalizers.

Section III, significant spectral broadening was observed at the signal channels near the ZDW but not in the longer wavelengths.

Fig. 15 plots the electrical SNR measured in each data channel after 9288 km transmission. All data channels offered SNRs above 21.6 dB (BER $<1 \times 10^{-9}$). We also note that there was no significant SNR degradation in the signal channels far from the zero-dispersion wavelength due to the proposed second- and third-order dispersion management technique.

VI. Conclusion

We have proposed a dispersion management technique for long-haul WDM transmission systems that reduces third-order dispersion with managing second-order dispersion to suppress the SPM-induced waveform distortion and interchannel interaction due to FWM and XPM. Its design method was described

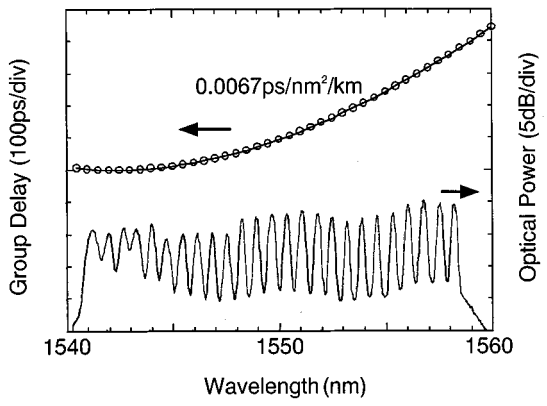

Fig. 14. Dispersion characteristics of the transmission line and the optical spectrum of the 25 × 10 Gb/s WDM signal measured after 9288 km transmission.

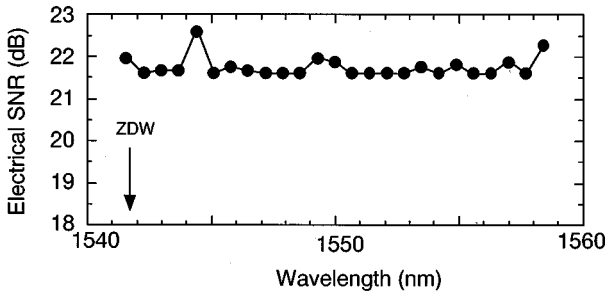

Fig. 15. Measured electrical SNR for 9288 km WDM transmission.

and experiments showed that the third-order dispersion averaged over the entire system could be reduced to about one-tenth that of a typical DSF, while local second-order dispersion was held to minus a few ps/nm/km.

A single-channel transmission experiment showed that the RZ format is superior to the NRZ format in the dispersion management line. Optimum RZ signal transmission performance was achieved in the anomalous dispersion region (in terms of the average value over the transmission line), wherein large SNR values and narrow spectral bandwidths were achieved over a wide wavelength range; to some extent this result might be due to the effect of nonlinearity in supporting RZ signal transmission. We also investigated the interchannel interaction in the transmission line. It was shown that FWM interaction was sufficiently small due to large local GVD value in the PDFs and NDFs. XPM was effectively reduced by coupling the signal channels with their polarization states orthogonal to each other. These results and gain equalization of over 16.8 nm allowed us to achieve 25 channel 10 Gb/s WDM transmission over 9288 km. The proposed technique is superior to conventional dispersion management in terms of performance and offers the possibility of further increases in transmission-capacity simply by increasing the optical amplifier bandwidth [13].

REFERENCES

[1] N. S. Bergano, C. R. Davidson, M. Ma, A. Pilipetskii, S. G. Evangelides, H. D. Kidorf, J. M. Darcie, E. Golovchenko, K. Rowitt, P. C. Corbett, R. Menges, M. A. Mills, B. Pedersen, D. Peckham, A. A. Abramov, and A. M. Vengsarkar, "320 Gb/s WDM transmission (64×5 Gb/s) over 7200 km using large mode fiber spans and chirped return-to-zero signals," in *Proc. OFC'98*, Postdeadline PD-12.

[2] M. Murakami, K. Suzuki, H. Maeda, T. Takahashi, A. Naka, N. Ohkawa, and M. Aiki, "High speed TDM-WDM techniques for long-haul submarine optical amplifier systems," *Optic. Fiber Technol.*, vol. 3, no. 4, pp. 320–338, 1997.

[3] G. P. Agrawal, *Nonlinear Fiber Optics*. New York: Academic.

[4] N. S. Bergano, C. R. Davidson, M. A. Mills, P. C. Corbett, R. Menges, J. L. Zyskind, J. W. Shulhoff, A. K. Srivastava, and C. Wolf, "Long-haul transmission using 10 Gb/s channels: A 160 Gb/s (16×10 Gb/s) 6000 km demonstration," in *Proc. OAA'97*, Postdeadline PD-9.

[5] K. Mukasa, Y. Akasaka, Y. Suzuki, and T. Kamiya, "Novel network fiber to manage dispersion at 1.55 mm with combination of 1.3 mm zero dispersion single mode fiber," *Proc. ECOC'97*, vol. 1, pp. 127–130, 1997.

[6] K. Yonenaga, A. Matsuura, S. Kuwahara, M. Yoneyama, Y. Miyamoto, K. Hagimoto, and K. Noguchi, "Dispersion-compensation-free 40-Gb/s'4 channel WDM transmission experiment using zero-dispersion-flattened transmission line," in *Proc. OFC'98*, Postdeadline PD-20.

[7] D. Marcuse, "RMS width of pulses in nonlinear dispersive fibers," *J. Lightwave Technol.*, vol. 10, pp. 17–21, Jan. 1992.

[8] A. Naka and S. Saito, "In-line amplifier transmission distance determined by self-phase-modulation and group-velocity-dispersion," *J. Lightwave Technol.*, vol. 12, pp. 280–287, Feb. 1994.

[9] Y. Yamamoto, ""Noise and error rate performance of semiconductor laser amplifiers in PCM-IM optical transmission systems," *IEEE J. Quantum Electron.*, vol. QE-16, no. 10, pp. 1073–1081, 1980.

[10] M. Murakami, T. Takahashi, M. Aoyama, T. Imai, M. Amemiya, M. Sumida, and M. Aiki, "System performance evaluation of the FSA submarine optical amplifier system," *J. Lightwave Technol.*, vol. 14, pp. 2657–2671, Dec. 1996.

[11] N. S. Bergano, F. W. Kerfoot, and C. R. Davidson, "Margin measurements in optical amplifier systems," *IEEE Photon. Technol. Lett.*, vol. 5, no. 3, pp. 948–951, 1991.

[12] M. Murakami, H. Maeda, T. Takahashi, N. Ohkawa, and T. Imai, "Transoceanic twelve 10 Gb/s WDM signal transmission experiment with individual dispersion and gain compensation and prechirped RZ pulse format," *Electron. Lett.*, vol. 33, no. 25, pp. 2145–2146, 1997.

[13] T. Matsuda, M. Murakami, and T. Imai, "340 Gb/s (34×10 Gb/s) WDM transmission over 8514 km using broadband gain equalization technique for transoceanic systems," *Electron. Lett.*, vol. 35, no. 13, pp. 1090–1091, 1999.

M. Murakami, photograph and biography not available at the time of publication.

T. Matsuda, photograph and biography not available at the time of publication.

H. Maeda, photograph and biography not available at the time of publication.

T. Imai, photograph and biography not available at the time of publication.